



1 **The role of the winter residual circulation in the summer mesopause**  
2 **regions in WACCM**

3 Maartje Sanne Kuilman<sup>1</sup>, Bodil Karlsson<sup>1</sup>

4 <sup>1</sup>Department of Meteorology, Stockholm University, 10691 Stockholm,  
5 Sweden.

6 *Correspondence to:* Maartje Kuilman ([maartje.kuilman@misu.su.se](mailto:maartje.kuilman@misu.su.se))

7  
8 **Abstract**

9  
10 High winter planetary wave activity warms the summer polar mesopause via a  
11 link between the two hemispheres. In a recent study carried out with the  
12 Kühlungsborn Mechanistic general Circulation Model (KMCM), it was shown  
13 that the net effect of this interhemispheric coupling mechanism is a cooling of  
14 the summer polar mesospheres and that this temperature response is tied to  
15 the strength of the gravity wave-driven winter mesospheric flow. We here  
16 reconfirm the hypothesis that the summer polar mesosphere would be  
17 substantially warmer without the circulation in the winter mesosphere, using  
18 the widely-used Whole Atmosphere Community Climate Model (WACCM). In  
19 addition, the role of the stratosphere in shaping the conditions of the summer  
20 polar mesosphere is investigated. Using composite analysis, we show that if  
21 winter gravity waves are absent, a weak stratospheric Brewer-Dobson  
22 circulation would lead to a warming of the summer mesosphere region instead  
23 of a cooling, and vice versa. This is opposing the temperature signal of the  
24 interhemispheric coupling in the mesosphere, in which a cold winter  
25 stratosphere goes together with a cold summer mesopause. We hereby  
26 strengthen the evidence that the equatorial mesospheric temperature  
27 response, driven by the winter gravity waves, is a crucial step in the  
28 interhemispheric coupling mechanism.

29  
30 **1 Introduction**

31  
32 The circulation in the mesosphere is driven by atmospheric gravity waves.  
33 These waves originate from the lower atmosphere and as they propagate  
34 upwards, they are filtered by the zonal wind in the stratosphere (e.g. Fritts and  
35 Alexander, 2003). Because of the decreasing density with altitude and as a



36 result of energy conservation, the waves grow in amplitude. At certain  
37 altitudes, the waves – depending on their phase speeds relative to the  
38 background wind - become unstable and break. At the level of breaking, the  
39 waves deposit their momentum into the background flow, creating a drag on  
40 the zonal winds in the mesosphere, which establishes the pole-to-pole  
41 circulation (e.g. Lindzen, 1981; Holton, 1982,1983; Garcia and Solomon,  
42 1985). This circulation drives the temperatures far away from the state of  
43 radiative balance, by adiabatically heating the winter mesopause and  
44 adiabatically cooling the summertime mesopause (Andrews et al., 1987;  
45 Haurwitz, 1961; Garcia and Solomon, 1985; Fritts and Alexander, 2003). The  
46 adiabatic cooling in the summer leads to temperatures sometimes lower than  
47 130 K in the summer mesopause (Lübken et al.,1990). These low  
48 temperatures allow for the formation of thin ice clouds in the summer  
49 mesopause region, the so-called noctilucent clouds (NLCs).

50  
51 Previous studies have shown that the summer polar mesosphere is influenced  
52 by the winter stratosphere via a chain of wave-mean flow interactions (e.g.  
53 Becker and Schmitz, 2003; Becker et al., 2004; Karlsson et al., 2009). This  
54 phenomenon, termed interhemispheric coupling (IHC), manifests itself as an  
55 anomaly of the zonal mean temperatures. Its pattern consists of a quadrupole  
56 in the winter hemisphere with a warming (cooling) of the polar stratosphere  
57 and an associated cooling (warming) in the equatorial stratosphere. Above in  
58 the mesosphere the temperature anomaly field is reversed with a cooling  
59 (warming) on top of the stratospheric warming (cooling) in the polar  
60 mesosphere, and an associated warming (cooling) in the equatorial region.  
61 The mesospheric warming (cooling) in the tropical region extends to the  
62 summer mesopause (see e.g. Körnich and Becker, 2010).

63  
64 The IHC pattern was first found using mechanistic models (Becker and  
65 Schmitz, 2003; Becker et al., 2004; Becker and Fritts, 2006), underpinned by  
66 observations of mesospheric conditions. The pattern was then found in  
67 observational data (e.g. Karlsson et al., 2007; Gumbel and Karlsson, 2011;  
68 Espy et al., 2011; de Wit et al., 2016), in the Whole Atmosphere Community  
69 Climate Model (WACCM: Sassi et al. 2004, Tan et al., 2012), in the Canadian



70 Middle Atmosphere Model (CMAM: Karlsson et al. 2009), and in the high  
71 altitude analysis from the Navy Operational Global Atmospheric Prediction  
72 System- Advanced Level Physics High Altitude (NOGAPS-ALPHA)  
73 forecast/assimilating system (Siskind et al., 2011).  
74  
75 The anomalies in the zonal-mean temperature fields are responses to  
76 different wave forcing in the winter hemisphere. A stronger planetary wave  
77 forcing in the winter stratosphere yields a stronger stratospheric Brewer-  
78 Dobson circulation (BDC). This anomalously strong flow yields an  
79 anomalously cold stratospheric tropical region and a warm stratospheric  
80 winter pole, due to the downward control principle (Haynes et al. 1991). The  
81 mechanism discussed here is for the case of a stronger winter residual  
82 circulation, but works the same for a weakening (Karlsson et al., 2009).  
83  
84 Due to the eastward zonal flow in the winter stratosphere, GWs carrying  
85 westward momentum propagate relatively freely up through the mesosphere  
86 where they break. Therefore, in the winter mesosphere, the net drag from  
87 GWs momentum deposition is westward. When vertically propagating  
88 planetary waves break – also carrying westward momentum – in the  
89 stratosphere, the momentum deposited onto the mean flow decelerates the  
90 stratospheric westerly winter flow. To put it short, a weaker zonal  
91 stratospheric winter flow allows for the upward propagation of more GWs with  
92 an eastward phase speed, which, as they break reduces the westward wave  
93 drag (see Becker and Schmitz, 2003, for a more rigorous description). This  
94 filtering effect of the zonal background flow on the GW propagation results in  
95 a reduction in strength of the winter-side mesospheric residual circulation  
96 when the BDC is stronger. The downward control principle now causes the  
97 mesospheric polar winter region to be anomalously cold and the tropical  
98 mesosphere to be anomalously warm (Becker and Schmitz, 2003, Becker et  
99 al., 2004; Körnich and Becker, 2009).  
100  
101 The critical step for IHC is the crossing of the temperature signal over the  
102 equator. The essential region is here the equatorial mesosphere. Central in  
103 the hypothesis of IHC is that the increase (or decrease) of the temperature in



104 the tropical mesosphere modifies the temperature gradient between high and  
105 low latitudes in the summer mesosphere, which influences the zonal wind in  
106 the summer mesosphere, due to thermal wind balance (see e.g. Karlsson et  
107 al., 2009 and Karlsson and Becker, 2016).

108 The zonal wind change in the summer mesosphere modifies the breaking  
109 level of the summer-side GWs. In the case of a warming in the equatorial  
110 mesosphere – as when the BDC is strong –, the zonal wind is modified in such  
111 a way that the intrinsic wave speeds are reduced (e.g. Becker and Schmitz,  
112 2003; Körnich and Becker, 2009). When the relative speed between the GWs  
113 and the zonal flow decreases, the GWs break at a lower altitude, thereby  
114 shifting down the GW drag per unit mass. The upper branch of the residual  
115 circulation also shifts downwards and along with this shift there is a reduction  
116 of adiabatic cooling, which causes a positive temperature anomaly in the  
117 summer mesosphere (Karlsson et al., 2009; Körnich and Becker, 2009;  
118 Karlsson and Becker, 2016). In the case of an equatorial mesospheric cooling,  
119 the response is the opposite: the relative difference between the zonal flow  
120 and the phase speeds of the gravity waves increase to that they break at a  
121 slightly higher altitude, with a anomalous cooling of the summer mesopause  
122 as a result.

123

124 The interhemispheric coupling mechanism is debated. For example,  
125 Pendlebury (2012) and Siskind and McCormack (2014) suggest the quasi-2  
126 day (Q2DW) wave to be involved in transferring the signal from the equatorial  
127 region to the summer polar mesopause region. They show that enhanced  
128 Q2DW activity leads to a warming of the summer mesopause. We argue that  
129 the Q2DW is an additional mechanism that comes into play controlling the  
130 summer mesospheric temperatures, adding to the effects of the IHC  
131 mechanism. A strong indication of it being two separate mechanisms – not  
132 necessarily unconnected – was presented by Karlsson and Becker (2016),  
133 who showed, using the Kühlungsborn Mechanistic general Circulation Model  
134 (KMCM), a more fundamental role of the interhemispheric coupling; the  
135 mechanism has a net cooling effect on the summer polar mesosphere. IHC  
136 has hitherto primarily been seen as a mode of internal variability giving rise to  
137 a warming of the summer polar mesopause region.



138

139 As mentioned above, the equatorial mesosphere is of crucial importance for  
140 interhemispheric coupling. The temperature in this region is modified by the  
141 strength of the residual circulation in the winter mesosphere. Karlsson and  
142 Becker (2016) hypothesized that if the GW-driven winter residual circulation  
143 would not be present, the equatorial mesosphere would be warmer, which  
144 would lead to lower breaking levels of GWs and a warmer summer  
145 mesosphere region. Analogically, an anomalously cold equatorial region  
146 would lead to an anomalously cold summer mesosphere region (e.g. Karlsson  
147 et al., 2009; Karlsson and Becker, 2016).

148

149 Becker and Karlsson (2016) showed that the equatorial mesosphere is  
150 substantially colder in July than it is in January, while the winter mesosphere  
151 is significantly warmer (see their Fig. 1). That means that the GWs break  
152 higher in the NH summer mesosphere than in the SH summer mesosphere,  
153 which is one possible reason for why the July summer polar mesosphere is  
154 colder than in the January summer polar mesosphere (e.g. Becker and Fritts,  
155 2006; Karlsson et al., 2009). If – as hypothesized by Karlsson and Becker  
156 (2016) – the fundamental effect of the IHC is a cooling of the summer  
157 mesopauses, it would mean that the mechanism plays a more important role  
158 affecting the temperatures in the summer mesopause in the NH compared to  
159 that in the SH, since the weaker planetary wave activity in the SH results in an  
160 increased gravity wave drag and a strengthening of mesospheric poleward  
161 flow in the winter mesosphere. The equatorial mesosphere would then be  
162 adiabatically cooled more efficiently than when the winter mesospheric  
163 circulation is weak. In the same manner, the NH winter has, in a climatological  
164 sense, a weaker effect on the residual circulation in the SH summer  
165 mesosphere, according to the mechanism described before.

166

167 Karlsson and Becker (2016) hypothesized that in the absence of the equator-  
168 to-pole flow in the SH winter, the summer mesopause in the NH would be  
169 considerably warmer. Moreover, removing the mesospheric residual  
170 circulation in the NH winter would not have as high impact on the SH summer  
171 mesopause. To test the hypothesis, they used the KMCM to compare control



172 simulations to runs without GWs in the winter mesosphere. The predicted  
173 responses were confirmed, and the results were also backed up by correlation  
174 studies using the Canadian Middle Atmosphere Model (CMAM30).

175

176 Since IHC is controversial, we find it important to use as many tools as  
177 possible to test – and to underpin - our arguments. In this study, the widely-  
178 used WACCM, described in Section 2.1 below, is used to endorse the results  
179 obtained with the not as widely-used – yet comprehensive – KMCM. To  
180 investigate the consequences for noctilucent clouds, formed in the  
181 mesopause region, of removing the winter mesospheric residual flow, we  
182 implement a basic cloud parameterization, as described in Section 2.2. The  
183 Whole Atmosphere Community Climate Model (WACCM) results from  
184 comparing runs with and without winter GWs are presented in Section 3. As  
185 an important complement to the study carried out by Karlsson and Becker  
186 (2016), we here examine the role of the summer stratosphere in shaping the  
187 conditions of the NH summer polar mesosphere when the winter mesospheric  
188 flow is absent. We focus on the effect that the zonal wind in the summer  
189 stratosphere has, and study if and how the PW activity in the winter affects  
190 the summer polar mesosphere. These results are presented in Section 3.1.  
191 Our conclusions are summarized in Section 4. Since the IHC mechanism has  
192 a more robust signal in the SH winter – NH summer, we choose to focus  
193 particularly on this period, namely July. Nevertheless, results from January  
194 are also shown for comparisons and for further discussion.

195

## 196 **2 Method**

197

### 198 **2.1 Model**

199

200 The Whole Atmosphere Community Climate Model (WACCM) is a so-called  
201 “high-top” chemistry-climate model, which spans the range of altitude from the  
202 Earth’s surface to an altitude of about 140 km. WACCM has 66 vertical levels  
203 of a resolution of ~1.1 km in the troposphere above the boundary layer, 1.1-  
204 1.4 km in the lower stratosphere, 1.75 km at the stratosphere and 3.5 km



205 above 65 km. The horizontal resolution is 1.9° latitude by 2.5° longitude  
206 (Marsh et al, 2013).

207

208 The model is a component of the Community Earth System Model (CESM),  
209 which is a group of model components at the National Center for Atmospheric  
210 Research (NCAR). WACCM is a superset of the Community Atmospheric  
211 Model version 4 (CAM4) and as such it includes all the physical  
212 parameterizations of CAM4 (Neale et al., 2013).

213

214 WACCM includes parameterized non-orographic gravity waves, which are  
215 generated by frontal systems and convection (Richter et al., 2010). The  
216 orographic GW parameterization is based on McFarlane (1987), while the  
217 nonorographic GW propagation parameterization is based the formulation by  
218 Lindzen (1981).

219

220 In this study, The F\_2000\_WACCM (FW) compset of the model is used, i.e.  
221 the model assumes present day conditions. There is no forcing applied: the  
222 model runs a perpetual year 2000. Our results are based on a control run and  
223 perturbation runs. In the control run, the winter side residual circulation is  
224 included. In the perturbation runs, the equator-to-pole flow is removed by  
225 turning off both the orographic and the non-orographic gravity waves. It  
226 should however be noted that even though the GWs are turned off, there are  
227 still some resolved waves, such as inertial gravity waves and planetary waves  
228 that drive a weak meridional circulation. The model is run for 30 years.

229

## 230 **2.2 Noctilucent clouds**

231 It was discussed earlier that the gravity-wave driven residual circulation in the  
232 middle atmosphere causes the temperatures in the summer mesopause  
233 region to be extremely low (e.g. Andrews et al., 1987), which allows for the  
234 formation of noctilucent clouds (NLCs) in this region. In the northern  
235 hemisphere, a typical NLC season lasts from late May until the end of August.  
236 In the southern hemisphere, the NLCs are present from the end of November  
237 until mid-February (e.g. Thomas and Olivero, 1989).



238 We parameterize these clouds in WACCM using the temperature and water  
239 vapor. We calculate the ice mass, assuming that water vapour can turn into  
240 ice if its partial pressure is larger than the saturation pressure. The saturation  
241 pressure is calculated using a fit to the numerical solution of the Clausius-  
242 Clapeyron equation, as derived by Murphy and Koop (2005). This model is  
243 based on the approach of Hervig et al. (2009).

244 Our method assumes that the ice exists in local thermodynamic equilibrium.  
245 This assumption has been shown to lead to an overestimation of the ice mass  
246 (e.g. Rong et al., 2010). Therefore, we assume that half of the water goes into  
247 ice, following a recent study by Christensen et al. (2016). We do not account  
248 for microphysical processes, as it has been shown before that NLCs can be  
249 modeled with very limited knowledge of their nucleation properties (Merkel  
250 et al., 2009; Megner et al., 2011).

### 251 **3 Results and discussion**

252 To investigate the effect of the winter residual circulation on the summer  
253 mesopause, we compare the control run, which includes the winter equator-  
254 to-pole circulation, with the perturbation runs. In the perturbation runs, the  
255 equator-to-pole flow is removed by turning off the parameterized gravity  
256 waves. The resolved waves, such as tides, inertial gravity waves and  
257 planetary waves are still there and drive a weak poleward flow, as already  
258 described in section 2.1.

259 We start by investigating the case for the NH summer (July) with the GWs  
260 turned off for the SH, where it is winter. Figure 1 shows the difference in  
261 zonal-mean temperature and zonal-mean zonal wind for July as a function of  
262 latitude and altitude, between the control run and the perturbation run: the run  
263 without the GWs in the winter minus the run with the GWs in the SH.

264 Figure 1.

265 From Fig. 1, it is clear that there is a considerable increase in temperature in  
266 the NH summer mesopause region in the case for which there is no equator-  
267 to-pole flow in the SH winter. Without the GWs in the SH winter, the winter



268 stratosphere and lower mesosphere are colder. This can be understood as  
269 GWs in the winter hemisphere drive downwelling, which adiabatically heats  
270 these regions. It is also clear that the zonal flow at high latitudes accelerates  
271 for the case for which there is no equator-to-pole flow in the SH winter. These  
272 findings correspond with what is found in Karlsson and Becker (2016).

273 It can also be seen that like in the KMCM model, the zonal wind and  
274 temperature in summer stratosphere region change only slightly in the  
275 perturbation runs as compared to the control runs. We deem that anomalous  
276 GW filtering effects from the lower down in the summer stratosphere, which  
277 could affect the results, are unlikely to contribute substantially to the  
278 temperature change in the summer mesosphere. We come back to this  
279 question in the next paragraph 3.1.

280 There is less upwelling in the NH summer mesopause in the case where the  
281 GWs in the SH winter hemisphere are turned off. We have seen that this  
282 leads to an increase in temperature in the summer mesopause, but at the  
283 same it leads to a decrease in water vapor concentration in the same region,  
284 as can be seen in Fig. 2. As a result of the increased temperature and  
285 decreased water vapor concentration, the noctilucent cloud ice mass density  
286 reduces, as is clear from Fig. 2.

287 Figure 2

288 The mechanism behind the reduction of the water vapor and the temperature  
289 increase is further illustrated in Fig. 3, which shows the zonal wind between  
290 45°N and 70°N, GW drag and temperature between 70°N and 90°N in July for  
291 the control and perturbation run. As a result of the changed meridional  
292 temperature gradient, the westward jet is weaker in the case in which there  
293 are no GWs in the winter hemisphere. The weaker jet, leads to lower GW  
294 levels and weaker GW drag as can be seen in Fig 3. Figure 3 also shows the  
295 temperature over the latitude bands 70° - 90° N, from this it can be seen that  
296 summer polar mesopause is considerably warmer if there are no GWs in the  
297 winter hemisphere.

298 Figure 3



299 To investigate the IHC mechanism further, we also show the correlation and  
300 covariance, which also provides information about the amplitude of the  
301 variability, between the temperature in the winter stratosphere in July (1-10  
302 hPa, 60°S-40°S) and the temperatures in the rest of the atmosphere in the  
303 same month. We show the correlation and covariance fields for both the  
304 cases with and without GWs in the SH winter hemisphere.

305 Figure 4

306 In the correlation and covariance fields of the control run, the temperature in  
307 the winter stratosphere is positively correlated with the temperature in the  
308 equatorial mesosphere and the summer mesopause region. If the GWs are  
309 removed in the winter hemisphere, the temperature in the summer  
310 mesopause region anti-correlates with the temperature in the winter  
311 stratosphere. Also, the temperature in the equatorial mesosphere does no  
312 longer correlate and co-vary significantly with the temperature in the winter  
313 hemisphere, in agreement with the results of Karlsson and Becker, 2016.

314 Until now, we investigated the influence of the SH winter residual circulation  
315 on the NH summer mesopause (in July). Now, we will also investigate the  
316 effect that the NH winter residual circulation has on the SH summer  
317 mesosphere (in January). We discussed earlier that this effect will be smaller  
318 as compared to the effect of the SH winter residual circulation on the NH  
319 summer mesosphere (in July). Figure 5 shows the difference in zonal-mean  
320 temperature and zonal-mean zonal wind for January as a function of latitude  
321 and altitude, between the control run and the perturbation run: the run without  
322 the GWs in the NH winter hemisphere minus the run with the GWs in the NH  
323 winter hemisphere.

324 Figure 5.

325 From Fig. 5, it can be observed that there is not such a clear increase in  
326 temperature in the SH summer mesopause region in the case for which there  
327 is no equator-to-pole flow in the NH winter. There is a small increase in the  
328 temperature for the upper part of the SH NLC region (January), but this  
329 change is not statistically significant. Without the GWs in the winter



330 hemisphere, the winter stratosphere and lower mesosphere are colder, as in  
331 the July case. There is a change in zonal wind at high southern latitudes, but  
332 there is no clear statistical significant increase. These findings correspond  
333 with what is hypothesized: the SH summer is less affected by the IHC  
334 mechanism.

335 In Fig. 6, we show the correlation and covariance between the temperature in  
336 the winter stratosphere in January (1-10 hPa, 60°S-40°S) and the  
337 temperatures in the rest of the atmosphere in the same month for both the  
338 cases with and without GWs in the NH winter hemisphere.

339 Figure 6

340 The general pattern in January for the correlation and covariance for both the  
341 control run and the run without GWs in the winter hemisphere is very similar  
342 to the pattern in July. However, the correlation and covariance in the summer  
343 mesosphere with the temperatures in the winter stratosphere are not  
344 statistically significant. This can be understood, as the variability in the SH  
345 summer mesopause region in January is much higher. It is seen that in both  
346 hemispheres, the temperature in the equatorial mesosphere correlates  
347 statistically significant with the temperatures in the winter stratosphere for the  
348 control case, but not for the case without the GWs in the winter hemisphere.

### 349 **3.1 The role of the summer stratosphere region**

350 In this section, we focus on the effect that the summer stratosphere has on  
351 the summer mesosphere in the absence of a mesospheric winter residual flow.  
352 We investigate if and how the planetary wave (PW) activity in the winter  
353 affects the summer polar mesosphere. We choose to focus particularly on the  
354 NH summer in July. However, we also show the effect of the SH summer  
355 stratosphere on the SH summer mesosphere in January for comparison and  
356 further discussion.

357

358 We start by looking at the control case in July, for which the GWs in the winter  
359 hemisphere are on. We use the temperature in the winter stratosphere (1-10  
360 hPa, 60°S-40°S; see Karlsson et al., 2007) as a proxy for the strength of the



361 Brewer-Dobson circulation and composite strong and weak cases. The  
362 anomalous temperature responses are shown in Fig. 7. It can be seen that  
363 when the temperature in the winter stratosphere region is anomalously low  
364 (high), there is a cooling (warming) of the NLC region.

365 Figure 7

366 The cold (warm) winter stratosphere is caused by an anomalously weak  
367 (strong) Brewer-Dobson circulation, which leads to a cooling (warming) of the  
368 equatorial mesosphere. This tropical temperature response changes the  
369 meridional temperature gradient in the summer mesosphere, and thereby –  
370 via thermal wind balance - the zonal mesospheric winds. The zonal wind  
371 change modifies the GW drag in such a way that a cooling (warming) of the  
372 NH summer mesopause is generated (see e.g. Karlsson et al. 2009). We note  
373 that a reversed meridional temperature gradient occurs simultaneously in the  
374 summer stratosphere as a response to the BDC. However, as pointed out by  
375 Karlsson et al. (2009), the expected GW filtering effect of this stratospheric  
376 temperature gradient would oppose that of the mesospheric temperature  
377 gradient.

378 With the mesospheric winter residual circulation being out of play, it is  
379 straight-forward to investigate effect of the temperature gradient in the  
380 summer stratosphere. Again, we show the anomaly fields for weak and strong  
381 stratospheric residual flow in the SH winter stratosphere (1-10 hPa, 60°S-  
382 40°S) in July, but this time without the winter GWs.

383 Figure 8

384 From Fig 8., it is clear that taking away the GWs in the SH winter hemisphere  
385 changes the response to anomalously high or low temperatures (i.e. high and  
386 low PW-activity, respectively: see e.g. Karlsson et al., 2007) in the summer  
387 mesopause region. Anomalously low temperatures in the SH winter  
388 stratosphere, indicating a weak Brewer-Dobson circulation, now lead to a  
389 warming in the NH summer mesopause region, instead of a cooling as  
390 observed in the case where there are GWs in the SH winter hemisphere.



391 We hypothesize that this opposing signal is – in the absence of a  
392 mesospheric residual flow in the winter - caused by a modulation of the  
393 meridional temperature gradient in the summer stratosphere, inferred by the  
394 BDC.

395 To strengthen our arguments, we plot the vertical profiles of the zonal wind,  
396 GW drag between 45°N-55°N and the temperatures between 70°N-90°N in  
397 July. These profiles are shown for both high and low temperatures in the  
398 winter stratosphere (1-10 hPa, 60°S-40°S). The differences between the  
399 cases with anomalously low and high temperatures are also plotted.

400 Figure 9

401 From Fig. 9, it is clear for a weak Brewer-Dobson circulation, and therefore  
402 anomalously low temperatures in the SH winter stratosphere, the zonal winds  
403 in the stratosphere are less strongly westwards. This leads to a weaker GW  
404 drag and a warmer NH summer mesopause region.

405 We hereby suggest that without GWs in the SH winter hemisphere, it would  
406 be the variability in the NH summer stratosphere caused by the winter-side  
407 BDC that would have the major influence on the temperatures in the NH  
408 summer mesopause. A weaker (stronger) Brewer-Dobson circulation would  
409 lead to a change in the temperature gradient in the summer stratopause,  
410 which would lead to a cooling (warming) instead of the warming (cooling)  
411 associated with interhemispheric coupling.

412 We also discuss the effect of the SH summer stratosphere on the SH summer  
413 mesosphere (in January). Also here, we start by looking at the control case, in  
414 which the GWs in the NH winter hemisphere are on.

415 We use the temperature in the winter stratosphere (1-10 hPa, 60°N-80°N) in  
416 January as a proxy for the strength of the Brewer-Dobson circulation and  
417 composite strong and weak cases. The anomalous temperature responses  
418 are shown in Fig. 10. In Fig. 6, we saw that the correlation of the temperatures  
419 with the winter stratosphere do not always reach a level of statistical  
420 significance of 95%. However, from Fig. 10 it is clear that the pattern is the



421 same as for the case in July: when the temperature in the winter stratosphere  
422 region is anomalously low (high), there is a cooling (warming) of the NLC  
423 region.

424 Figure 10

425 Like we did for the July case, we show the anomaly fields for weak and strong  
426 stratospheric residual flow in the winter stratosphere (1-10 hPa, 60°N-80°S) in  
427 January, for the case without the winter GWs.

428 Figure 11

429 From Fig 11., it is clear that also for the January, taking away the GWs in the  
430 winter hemisphere leads to a different response to anomalously high or low  
431 temperatures in the winter stratosphere as compared to the control case. As  
432 in the July, anomalously low temperatures in the winter stratosphere  
433 (associated with a weak Brewer-Dobson circulation) lead to a warming in the  
434 summer mesopause region, instead of a cooling for the case where there are  
435 GWs in the winter hemisphere.

436 In Fig. 12, we show the vertical profiles of the zonal wind, GW drag between  
437 45°S-55°S and the temperatures between 70°S-90°S for both high and low  
438 temperatures in the winter stratosphere (1-10 hPa, 40°N-60°N, January). In  
439 addition, the differences between the cases with anomalously low and high  
440 temperatures are shown.

441 Figure 12

442 The profiles for the southern hemisphere in January are very similar to the  
443 profiles for the northern hemisphere in July. Also here, for a weak Brewer-  
444 Dobson circulation, the zonal winds in the stratosphere are less strongly  
445 westwards, leading to a weaker GW drag and a warmer summer mesopause  
446 region. To summarize, both in the northern and summer hemisphere, a  
447 weaker (stronger) Brewer-Dobson circulation leads to a change in the  
448 temperature gradient in the summer stratopause, which leads to a warming  
449 (cooling) instead of the cooling (warming) that is associated with



450 interhemispheric coupling.

#### 451 **4 Conclusions**

452 In this study, the interhemispheric coupling mechanism and the role of the  
453 summer stratosphere in shaping the conditions of the summer polar  
454 mesosphere have been investigated. We have used the widely used WACCM  
455 model to reconfirm the hypothesis of Karlsson and Becker (2016) that the  
456 summer polar mesosphere would be substantially warmer without the gravity  
457 wave-driven residual circulation in the winter. We find, in accordance with the  
458 previous study, that the interhemispheric coupling mechanism has a net  
459 cooling effect on the summer polar mesospheres. We also find that the  
460 mechanism plays a more important role affecting the temperatures in the  
461 summer mesopause in the NH compared to that in the SH.

462

463 We have also investigated the role of the summer stratosphere in shaping the  
464 conditions of the summer polar mesosphere. It is shown that without the  
465 winter mesospheric residual circulation, the variability in the summer polar  
466 mesosphere is determined by the temperature gradient in the summer  
467 stratosphere below, which is modulated by the strength of the BDC. We have  
468 found that for both the northern and the southern hemisphere, in the absence  
469 of winter gravity waves, a weak Brewer-Dobson circulation would lead to a  
470 warming of the summer mesosphere region. The temperature signal of the  
471 interhemispheric coupling mechanism is opposite: in this case a weak Brewer-  
472 Dobson circulation, the summer mesosphere region is cooled. This confirms  
473 the idea that it is the equatorial mesosphere that is governing the  
474 temperatures in the summer mesopause regions, rather than processes in the  
475 summer stratosphere.

476

477

478

479

480

481

482

483

484



485 **References**

- 486  
487 Andrews, D.G., Holton, J.R., Leovy, C.B.: Middle atmosphere dynamics,  
488 Academic Press, United States of America, 1987.  
489  
490 Becker E. and Fritts, D.C.: Enhanced gravity-wave activity and  
491 interhemispheric coupling during the MacWAVE/MIDAS northern summer  
492 program 2002, Ann. Geophys., 24, 1175-1188, doi:10.5194/angeo-24-1175-  
493 2006, 2006.  
494  
495 Becker, E. and Schmitz, G.: Climatological effects of orography and land-sea  
496 contrasts on the gravity wave-driven circulation of the mesosphere, J. Atmos.  
497 Sci., 60, 103-118, doi:10.1175/1520-0469(2003)060<0103:CEOAL>2.0.CO;2,  
498 2003.  
499  
500 Becker, E., Müllermann, A., Lübken, F.-J., Körnich, H., Hoffmann, P., Rapp,  
501 M.: High Rossby-wave activity in austral winter 2002: Modulation of the  
502 general circulation of the MLT during the MacWAVE/MIDAS northern summer  
503 program, Geophys. Res. Lett., 31, L24S03, doi:10.1029/2004GL019615, 2004.  
504  
505 Christensen, O.M., Benze, S., Eriksson, P., Gumbel, J., Megner, L., Murtagh,  
506 D.P.: The relationship between Polar Mesospheric Clouds and their  
507 background atmosphere as observed by Odin-SMR and Odin-OSIRIS, Atmos.  
508 Chem. Phys., 16, 12587-12600, doi:10.5194/acp-16-12587-2016, 2016.  
509  
510 De Wit, R.J., Janches, D., Fritts, D.C., Hibbins, R.E.: QBO modulation of the  
511 mesopause gravity wave momentum flux over Tierra del Fuego, Geophys.  
512 Res. Lett., 43, 4094-4055, doi:10.1002/2016GL068599, 2016.  
513  
514 Espy, P.J., Ochoa Fernández, S., Forkman, P., Murtagh, D., Stegman, J.:  
515 The role of the QBO in the inter-hemispheric coupling of summer mesospheric  
516 temperatures, Atmos. Chem. Phys., 11, doi:10.5194/acp-11-495-2011, 495-  
517 502, 2011.  
518  
519 Fritts, D. C. and Alexander, M.J.: Gravity wave dynamics and effects in the



- 518 middle atmosphere, *Rev. Geophys.*, 41, 1003, doi:10.1029/2001RG000106,  
519 2003.  
520
- 521 Garcia, R.R., Solomon, S.: The effect of breaking gravity waves on the  
522 dynamics and chemical composition of the mesosphere and lower  
523 thermosphere, *J. Geophys. Res.*, 90, D2, 3850-3868,  
524 10.1029/JD090iD02p03850, 1985.  
525
- 526 Gumbel, J., Karlsson, B.: Intra- and inter-hemispheric coupling effects on the  
527 polar summer mesosphere, *Geophys. Res. Lett.*, 38, L14804,  
528 doi:10.1029/2011GL047968, 2011.  
529
- 530 Haurwitz, B.: Frictional effects and the meridional circulation in the  
531 mesosphere, *J. Geophys. Res.*, 66, 8, doi:10.1029/JZ066i008p02381, 1961.  
532
- 533 Haynes, P.H., Marks, C.J., McIntyre, M.E., Shepherd, T.G., Shine, K.P.: On  
534 the “downward control” of extratropical diabatic circulations by eddy-induced  
535 mean zonal forces, *J. Atmos. Sci.*, 48, 651-678, 10.1175/1520-  
536 0469(1991)048<0651:OTCOED>2.0.CO;2, 1991.
- 537 Hervig, M.E., Stevens, M.H., Gordley, L.L., Deaver, L.E., Russell, J.M., Bailey,  
538 S.M.: Relationships between polar mesospheric clouds, temperature, and  
539 water vapor from Solar Occultation for Ice Experiment (SOFIE) observations,  
540 *J. Geophys. Res.*, 114, D20203, doi:10.1029/2009JD012302, 2009.
- 541 Holton, J.R.: The role of gravity wave induced drag and diffusion in the  
542 momentum budget of the mesosphere, *J. Atmos. Sci.*, 39, 791-799,  
543 doi:10.1175/1520-0469(1982)039<0791:TROGWI>2.0.CO;2, 1982.  
544
- 545 Holton, J.R.: The influence of gravity wave breaking on the general circulation  
546 of the middle atmosphere, *J. Atmos. Sci.*, 40, 2497-2507, doi:10.1175/1520-  
547 0469(1983)040<2497:TIOGWB>2.0.CO;2, 1983.  
548
- 549 Karlsson, B., Körnich, H., Gumbel, J.: Evidence for interhemispheric



- 550 stratosphere-mesosphere coupling derived from noctilucent cloud properties,  
551 Geophys. Res. Lett., 34, L16806, doi:10.1029/2007GL030282, 2007.  
552
- 553 Karlsson, B., McLandress, C., Shepherd, T.G.: Inter-hemispheric mesospheric  
554 coupling in a comprehensive middle atmosphere model, J. Atmos. Sol.-Terr.  
555 Phys., 71, 3-4, 518-530, doi:10.1016/j.jastp.2008.08.006, 2009.  
556
- 557 Karlsson, B., Becker, E.: How does interhemispheric coupling contribute to  
558 cool down the summer polar mesosphere?, 29, 8807-8821, doi:10.1175/JCLI-  
559 D-16-0231.1, J. Climate, 2016.  
560
- 561 Körnich, H. and Becker, E.: A simple model for the interhemispheric coupling  
562 of the middle atmosphere circulation, Adv. in Space Res., 45, 5, 661-668,  
563 doi:10.1016/j.asr.2009.11.001, 2010.  
564
- 565 Lindzen, R.S.: Turbulence stress owing to gravity wave and tidal breakdown,  
566 J. Geophys. Res., 86, C10, 9707-9714, 10.1029/JC086iC10p09707, 1981.  
567
- 568 Lübken, F.-J., Von Zahn, U., Manson, A., Meek, C., Hoppe, U.-P., Schmidlin,  
569 F.J., Stegman, J., Murtagh, D.P., Rüster, R., Schmitz, G., Widdel, H.-U., Espy,  
570 P.: Mean state densities, temperatures and winds during the MAC/SINE and  
571 MAC/EPSILON campaigns, J. Atmos. Sol.-Terr. Phys., 52, 10-11, 955-970,  
572 [https://doi.org/10.1016/0021-9169\(90\)90027-K](https://doi.org/10.1016/0021-9169(90)90027-K), 1990.  
573
- 574 Pendlebury, D.: A simulation of the quasi-two-day wave and its effect on  
575 variability of summertime mesopause temperatures, J. Atmos. Sol.-Terr.  
576 Phys., 80, 138-151, doi: 10.1016/j.jastp.2012.01.006, 2012.
- 577 Richter, J. H., Sassi, F., Garcia, R.R.: Toward a physically based gravity wave  
578 source parameterization in a general circulation model, J. Atmos. Sci., 67,  
579 136–156, DOI: 10.1175/2009JAS3112.1, 2010.
- 580 Rong, P., Russell, J. M., Gordley, L. L., Hervig, M. E., Deaver, L., Bernath, P.  
581 F., Walker, K. A.: Validation of v1.022 mesospheric water vapor observed by



582 the Solar Occultation for Ice Experiment instrument on the Aeronomy of Ice in  
583 the Mesosphere satellite, *J. Geophys. Res.*, 115, D24314,  
584 doi:10.1029/2010JD014269, 2010.

585  
586 Marsh, D. R., Mills, M.J., Kinnison, D.E., Lamarque, J.F., Calvo, N., Polvani,  
587 L.M.: Climate change from 1850 to 2005 simulated in CESM1(WACCM),  
588 73727391, *J. Climate*, 26, 19, doi:10.1175/JCLI-D-12-00558.1, 2013.

589 McFarlane, N. A.: The effect of orographically excited wave drag on the  
590 general circulation of the lower stratosphere and troposphere, *J. Atmos. Sci.*,  
591 44, 1775–1800, 10.1175/1520-0469(1987)044<1775:TEOOEG>2.0.CO;2,  
592 1987.

593 Megner, L.: Minimal impact of condensation nuclei characteristics on  
594 observable mesospheric ice properties, *J. Atmos. Sol.-Terr. Phys*, 73, 14-15,  
595 2184-2191, doi:10.1016/j.jastp.2010.08.006, 2011.

596  
597 Merkel, A.W., Marsh, D.R., Gettelman, A., Jensen, E.J: On the relationship of  
598 polar mesospheric cloud ice water content particle radius and mesospheric  
599 temperature and its use in multi-dimensional model, *Atmos. Chem. Phys.*, 9,  
600 8889-8901, doi:10.5194/acp-9-8889-2009, 2009.

601  
602 Murphy, D. M. and Koop, T.: Review of the vapor pressure of ice and super-  
603 cooled water for atmospheric applications, *Q. J. R. Meteorol. Soc.*, 131, 1539-  
604 1565, doi:10.1256/qj.04.94, 2005.

605 Neale, R., Richter, J., Park, S., Lauritzen, P., Vavrus, S., Rasch, P., Zhang,  
606 M.: The mean climate of the Community Atmosphere Model (CAM4) in forced  
607 SST and fully coupled experiments, *J. Climate*, 26, 5150–5168,  
608 doi:10.1175/JCLI-D-12-00236.1, 2013.

609 Sassi, F., Kinnison, D., Boville, B.A., Garcia, R.R., Roble, R.: Effect of El  
610 Niño- Southern Oscillation on the dynamical, thermal, chemical structure of  
611 the middle atmosphere, *J. Geophys. Res.*, 109, D17108,



612 doi:10.1029/2003JD004434, 2004.

613

614 Siskind, D. E., Stevens, M.H., Hervig, M., Sassi, F., Hoppel, K., Englert, C.R.,

615 Kochenas, A.J., Consequences of recent Southern Hemisphere winter

616 variability on polar mesospheric clouds, *J. Atmos. Sol. Terr. Phys.*, 73, 2013–

617 2021, 10.1016/j.jastp.2011.06.014, 2011.

618

619 Siskind, D.E. and McCormack, J.P.: Summer mesospheric warmings and the

620 quasi 2 day wave, *Geophys. Res. Lett.*, 41, 717-722, doi:10.1002/

621 2013GL058875, doi:10.1016/j.jastp.2011.06.014, 2014.

622

623 Tan, B., Chu, X., Liu, H.-L.: Yamashita, C., Russell III, J.M.: Zonal-mean

624 global teleconnections from 15 to 110 km derived from SABER and WACCM,

625 *J. Geophys. Res.*, 117, D10106, doi:10.1029/2011JD016750, 2012.

626

627 Thomas, G. E., Olivero, J.J.: Climatology of polar mesospheric clouds 2.

628 Further analysis of Solar Mesosphere Explorer data, *J. Geophys. Res.*, 96,

629 14673-14681, doi:10.1029/JD094iD12p14673, 1989.

630

631

632

633

634

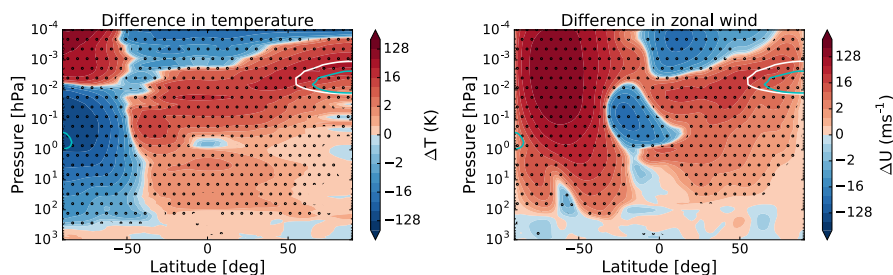
635

636

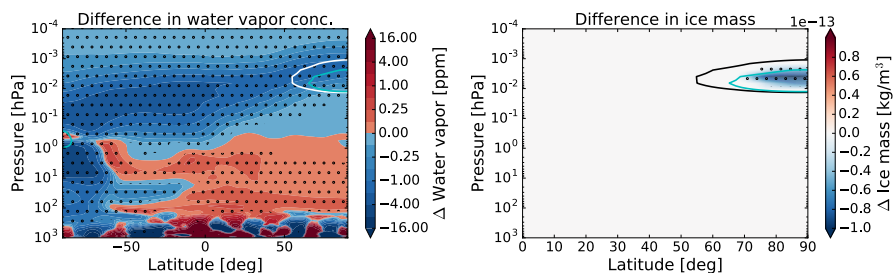
637

638

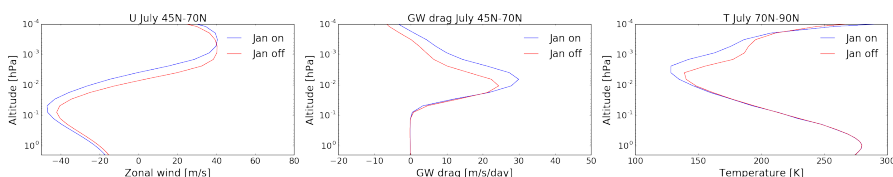
639



640  
 641 Fig. 1. The difference in zonal-mean temperature (left) and zonal-mean  
 642 zonal wind (right) for July: [run without winter GWs] minus [control run]. The white  
 643 contour indicates the summer polar mesopause region where the  
 644 temperatures are below 150 K for the control run. The blue contour indicates  
 645 the region where the temperature is below 150 K for the run without the GWs  
 646 in winter. The dotted areas are regions where the data reaches a confidence  
 647 level of 95%.



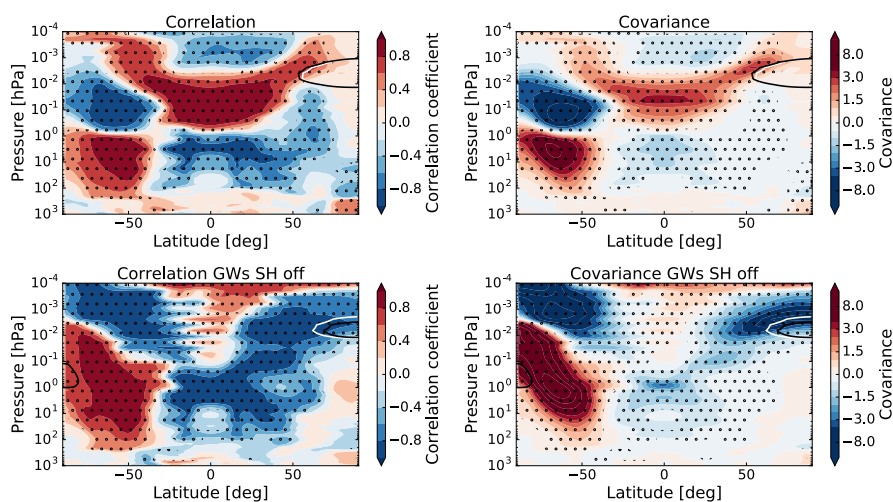
648  
 649 Fig. 2. The difference in zonal-mean water vapour concentration (left) and  
 650 zonal-mean ice mass density (right) for July: [run without winter GWs] minus  
 651 [control run]. The black contour indicates the region where the temperatures is  
 652 below 150 K for the control run. The blue contour indicates the region where  
 653 the temperature is below 150 K for the run without the GWs in winter. The  
 654 dotted areas are regions where the data reaches a confidence level of 95%.



655  
 656 Fig. 3. Interhemispheric coupling in July, illustrated by the zonal wind and the  
 657 GW drag between 45° and 70° N and the temperature between 70° and 90° N.

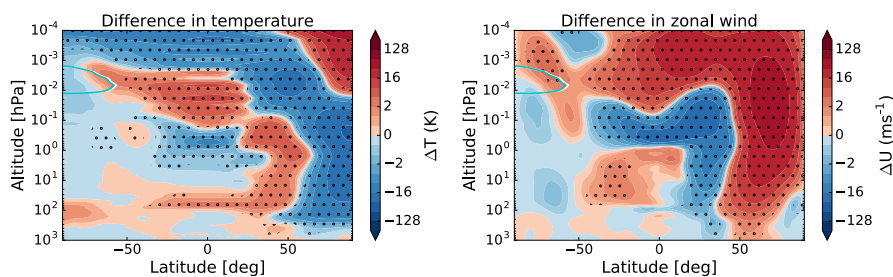


658 The blue lines show the control run and the red lines show the run without  
659 GWs in the winter hemisphere.



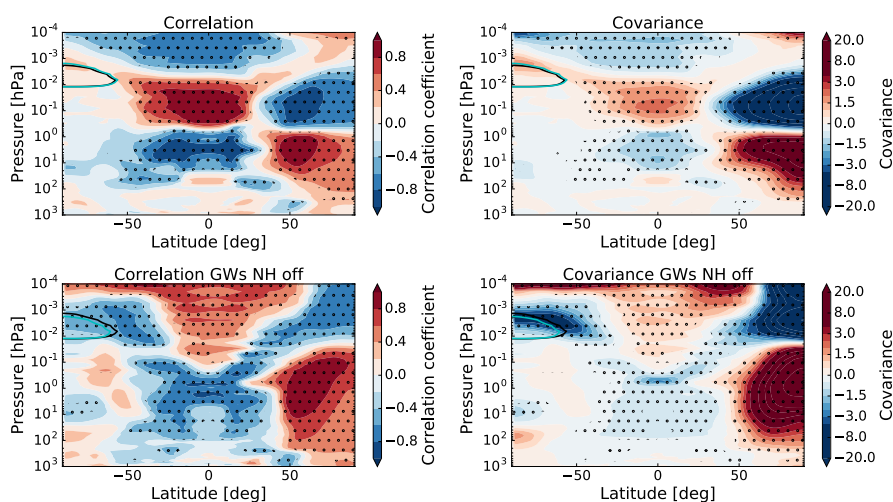
660

661 Fig. 4. The correlation (left) and covariance (right) between the temperature in  
662 the winter stratosphere (1-10 hPa, 60°S-40°S) and the temperatures in the  
663 rest of the atmosphere in July for the control run (first row) and run without  
664 GWs in the winter hemisphere (bottom row). The dotted areas are regions  
665 where the correlation has a p-value < 0.05. The black and the blue 150 K-  
666 contour indicate the polar mesopause region.



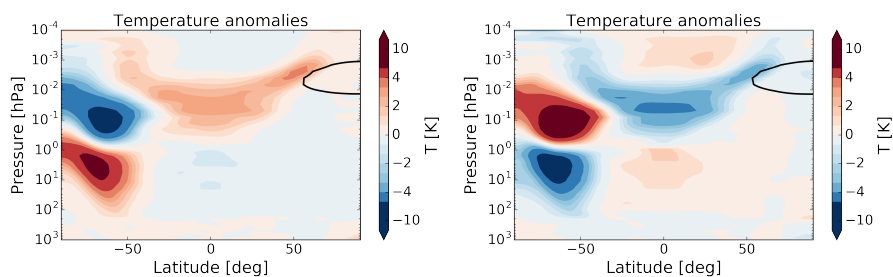
667  
668

Fig. 5. Same as Figure 1, but for January.



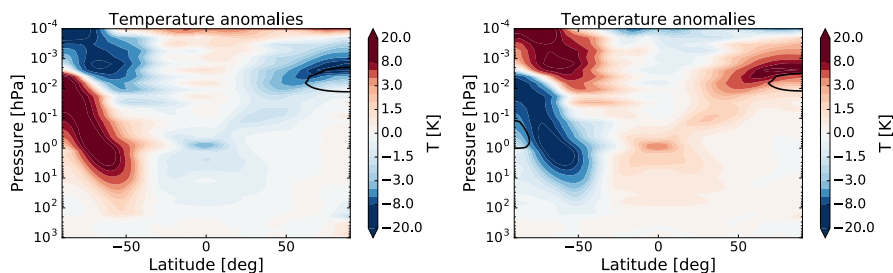
669

670 Fig. 6. The correlation (left) and covariance (right) between the temperature in  
671 the winter stratosphere (1-10 hPa, 40°N-60°N) and the temperatures in the  
672 rest of the atmosphere in January for the control run (first row) and run without  
673 GWs in the winter hemisphere (bottom row). The black and the blue 150 K-  
674 contour indicate the polar mesopause region. The dotted areas are regions  
675 where the correlation has a p-value < 0.05.



676

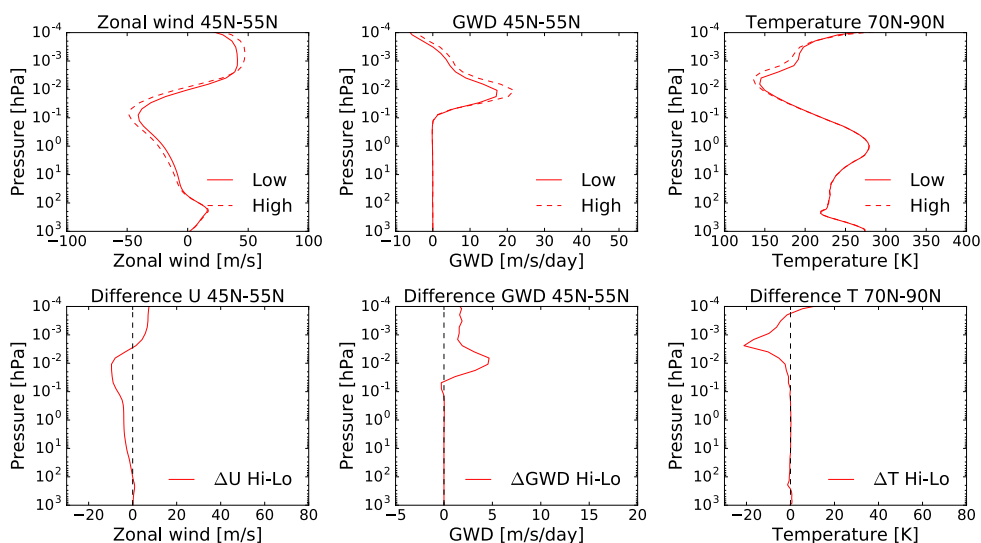
677 Fig. 7. The July temperature anomalies for anomalously high (left) and low  
678 (right) temperatures in the winter stratosphere (1-10 hPa, 60°S-40°S) for the  
679 control run. The black 150 K-contour indicates the polar mesopause region



680

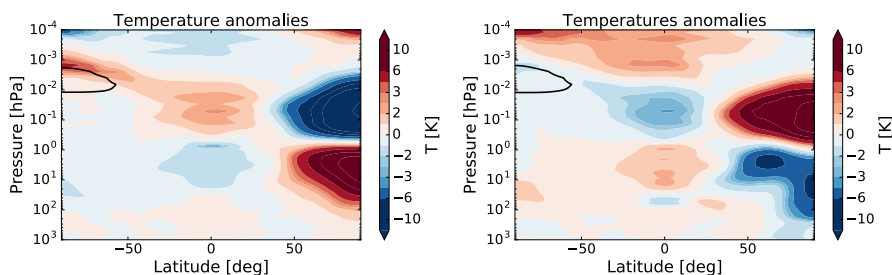


681 Fig. 8. The July temperature anomalies for anomalously high (left) and low  
 682 (right) temperatures in the winter stratosphere (1-10 hPa, 60°S-40°S) for the  
 683 run without GWs in the winter hemisphere. The black 150 K-contour indicates  
 684 the polar mesopause region.



685

686 Fig. 9. The July zonal wind (left) and the GW drag (middle) between 45°-  
 687 55°N and the temperature (right) between 70-90°N for anomalously low and  
 688 high temperatures in the winter stratosphere (1-10 hPa, 60°S - 40°S) (first  
 689 row) and the differences between them (second row), for the case where  
 690 there are no GWs in the winter hemisphere. The red continuous lines show  
 691 the results for anomalously low temperatures, the red dotted lines show the  
 692 results for the anomalously high temperatures.

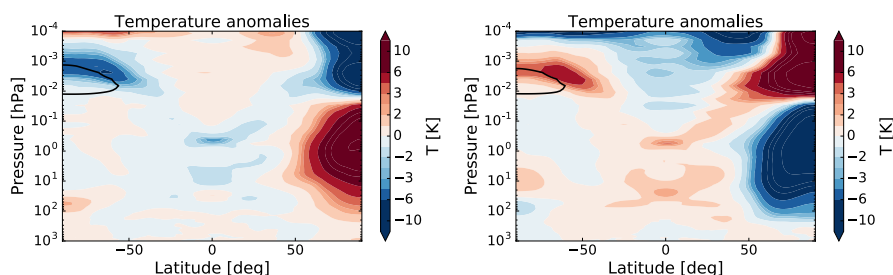


693

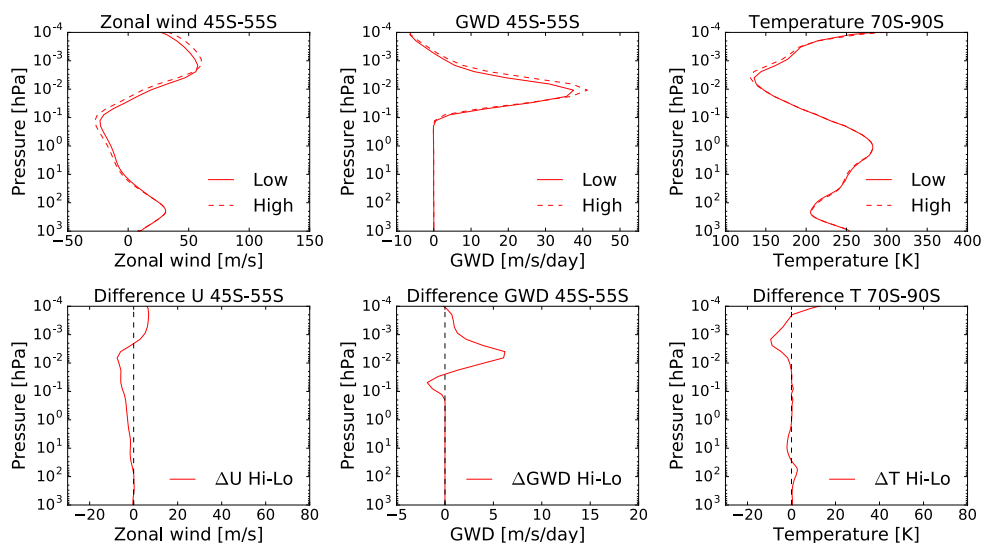
694 Fig. 10. The January temperature anomalies for anomalously high (left) and  
 695 low (right) temperatures in the winter stratosphere (1-10 hPa, 40°N-60°N) for



696 the control run. The black 150 K-contour indicates the polar mesopause  
 697 region.



698  
 699 Fig. 11. The January temperature anomalies for anomalously high (left) and  
 700 low (right) temperatures in the winter stratosphere (1-10 hPa, 40°N-60°N) for  
 701 run without GWs in the winter hemisphere. The black 150 K-contour indicates  
 702 the polar mesopause region.



703  
 704 Fig. 12. The January zonal wind (left) and the GW drag (middle) between 45°-  
 705 55°S and the temperature (right) between 70°S-90°S for anomalously low and  
 706 high temperatures in the winter stratosphere (1-10 hPa, 40°N - 60°N) (first  
 707 row) and the differences between them (second row), for the case where  
 708 there are no GWs in the winter hemisphere. The red continuous lines show  
 709 the results for anomalously low temperatures, the red dotted lines show the  
 710 results for the anomalously high temperatures.